Gradient-Based Repetitive Learning Control for Rotor Vibration Control

Kari TAMMI

Abstract- **Repetitive learning control was examined for active vibration control of rotor. A novel modification of a gradient-based repetitive learning control algorithm was developed. The stability of the algorithm was studied and the algorithm was tested on a rotor test rig. The experiments showed that repetitive learning control attenuated efficiently rotor vibrations excited by rotor unbalances. In addition to experimental work, the paper presents convergence and stability properties of the proposed repetitive learning control approach.**

Index Terms—**active vibration control, repetitive control, learning control, rotor, rotating machine**

1. INTRODUCTION

Active vibration control is making its debut in machine industry. Traditionally, typical applications have been found in aerospace and precision engineering. Active control of rotor and rotor-induced vibrations is becoming more common together with tightening requirements on vibrations and noise emitted. Different types of adaptive feedforward algorithms have been studied to attenuate rotation induced vibrations [6, 5]. Our aim is to study what may be achieved with repetitive learning control in the context of rotor radial vibration control. The current paper reports the results achieved with repetitive learning control. A more covering comparative study of different control approaches can be found in [16]. The novelty of this paper is in the experimental application of repetitive learning control on variable-speed rotating machines. Repetitive control has been applied on rotating machines before [14, 18], but variable speed machines and digital control systems pose additional challenges as it is shown below. This paper suggests an interpolation method and DC removal method to compensate disturbances with variable period. Also, this paper shows a method to study stability of repetitive controller on complex plane and to relate it to windowing techniques in data acquisition. The method is originally published in [1].

1.1 Repetitive Learning Control for Rotor Vibrations

The internal model principle states that a system has to contain a model of a signal in order to track or compensate the signal perfectly [2]. This idea has been utilized in the compensation of rotation harmonics in rotor vibration control. In feedforward systems, the model of the signal is in the form of a reference signal. In the repetitive and iterative learning control systems, the signal is learnt by means of a delay line with positive feedback. The original idea of repetitive control was presented by Inoue *et al.* for high accuracy control of a magnet power supply [11]. The aim is to develop a controller that tracks a periodic control signal. The use of positive feedback and a delay line makes it possible to track the control signal perfectly. This property makes repetitive control an attractive solution for compensation of periodic disturbance signals. Figure 1 shows a basic disturbance compensation scheme with a repetitive controller (the disturbance is $d(s)$, where s is the Laplace variable). The magnitude of the output error, $e(s)$, to be minimized, is fed back. Also, the old control outputs are delayed by time T and fed back, with a positive loop gain. This leads to a control law where controller outputs are updated (taught) by the realized output errors
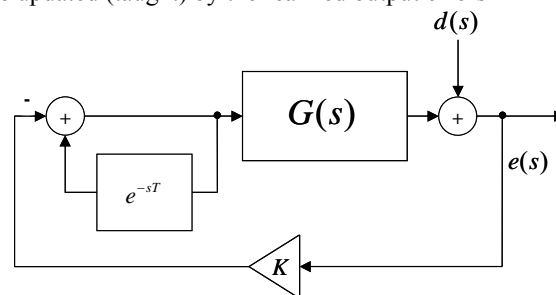

Figure 1. The basic scheme of the repetitive control.

Figure 2 shows a simulation example carried out on the system in Figure 1 with $G(s) = 1$. The delay time T is set such that it matches the frequency components in the disturbance signal ($1/T$ and $2/T$). The control signal is learnt during about eight periods in such away that the output error $e(t)$ is driven to zero (t is the time variable).
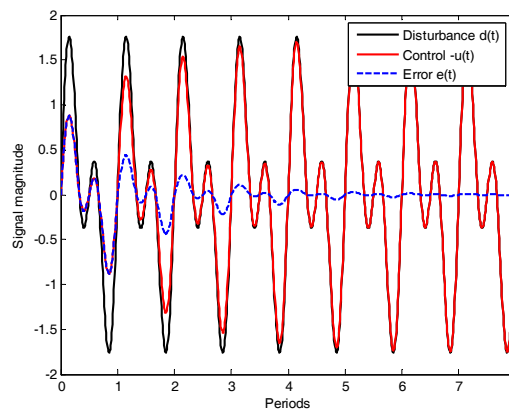

Figure 2. Simulation example of the basic repetitive controller. The signals are plotted against the fundamental period of the disturbance (1/T).

Manuscript received November 1, 2008. The manuscript has been partially published in the doctoral thesis of the author [16].

Kari Tammi is with VTT – Technical Research Centre of Finland, P.O.Box 1000, FI-02044 VTT, Finland. (e-mail: kari.tammi@vtt.fi).

Potential solutions for repetitive learning control have been found in tracking or compensation problems [13, 8], in robotics [3], in computer disk drives [18, 12, 15], in peristaltic pumps [8], *etc.* A periodic disturbance, often due to rotary movement, can be found as the common denominator behind the applications.

As explained above, repetitive controllers were developed to track or to compensate periodic signals. The idea behind the repetitive control method is to continuously refine the control output by using old control outputs and error data. The control law in continuous time, as its simplest, is

$$u(t) = u(t-T) - Ke(t) \qquad (1)$$

where $u(t)$ are the control outputs, $e(t)$ is the error quantity and T is the delay time, and K is the feedback gain. The delay time is to be set equal to the period of the signal to be tracked or compensated. Positive feedback of the delayed signal leads to high, ideally infinite, feedback gain at frequencies matching the inverse of the delay time

$$f = \frac{n}{T} \qquad (2)$$

where n is a non-negative integer corresponding to the harmonic number. A sufficient condition for stability of the repetitive controller is that the system loop gain must be positive real, because of the high feedback loop gain. In Figure 3, the loop gain is plotted against the harmonic number (n). The requirement of positive realness can be understood by considering the denominator of the closed-loop system with repetitive controller

$$H_{rep}(s) = \frac{u(s)}{d(s)} = \frac{-K}{1 - e^{-sT} + KG(s)} \qquad (3)$$

where $KG(s)$ represents the loop gain transfer function of the system. The real part of the $KG(s)$ must be positive in order to maintain the stability (to prevent the denominator from being zero). In other words, the phase of $KG(s)$ must be within ±90°. These requirements guarantee stability, because positive real systems can tolerate infinite feedback gain. The result can also be understood by considering the classical Nyquist stability criterion that states that the loop gain must not encircle the point (–1, i 0) in the complex plane. If $KG(i\omega)$ has a positive real part, it cannot encircle the point, regardless of the feedback gain. Note again that the requirement stated is a sufficient condition for stability and less conservative requirements exist. The requirement of positive realness is relatively stringent for mechanical systems, which often have resonances and anti-resonances, where phase changes often exceed 90°.

The basic repetitive controller was presented above using the continuous time formulation. Moving to the discrete time domain may ruin the controller stability, since sampled systems are rarely positive real. It has been shown that a discrete system can be a positive real system only if the system's output is directly influenced by the

inputs, *i.e.*, the direct term in the state-space representation is not equal to zero [9]. As known, the direct term is frequently equal to zero in practical systems with finite sampling frequency. This can be understood by considering the signal delay due to sampling. The phase lag of a sampled and reconstructed signal with respect to the actual continuous-time signal grows as the Nyquist frequency is approached.
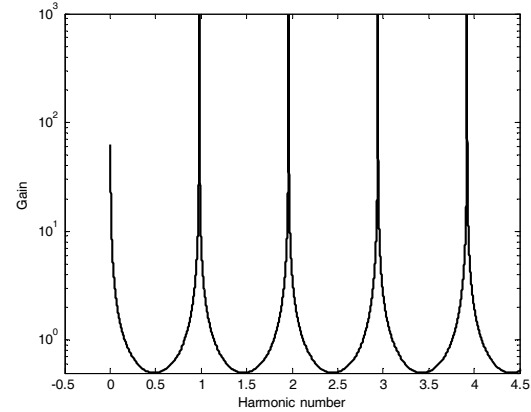

Figure 3. The loop gain of a repetitive controller.

Because several practical control systems are implemented digitally and operate in discrete time, the repetitive control theory has been developed in the discrete time domain, respectively. In order to tune stability and convergence characteristics, the basic repetitive control law in Eq. (1) has been modified to contain pre-filters for the old-control (learning) component and for the control error component

$$u(n) = Q(q)q^{-N}u(n) + K(q)e(n) \qquad (4)$$

where $Q(q)$ is a filter or a constant number and $K(q)$ is the feedback gain, also a filter or a constant number, and q is the forward shift operator with q^{-N} representing a backward shift of N samples. Filter $Q(q)$, which has a gain of less or equal to unity, has been used for restricting the control actions to a desired frequency band. It will later be referred to as the *Q filter*. The filter $K(q)$ has been used to appropriately modify the loop gain $K(q)G(q)$ [18]. At least, it means having the loop gain positive real at the frequencies where abs(Q) ≈ 1. As will be shown, the delay line gives more freedom in the design of $K(q)$; it actually provides an opportunity for a non-causal implementation that makes a zero-phase-lag filter possible.

2. MATERIALS AND METHODS

2.1 Test Rig for Rotor Vibration Control

The experiments were carried out on a laboratory test rig. The test environment had a 560-mm long slim shaft with three disks attached (Figures 4 and 5). The disks were fixed to the shaft to make it resemble a real-life machine and to tailor the dynamics of the shaft. The disk locations

were chosen in such a way that the rotor exhibited a speed-dependent behavior, although the speed-dependence was later found rather weak. The total weight of the rotor including the shaft and three disks was 2.7 kg. The rotor was supported by two journal bearings, 360 mm apart. An electro-magnetic actuator was located at the non-drive end of the rotor whereas the vibrations were to be attenuated inside the bearing span of the rotor. Radial displacement sensors were situated at two locations along the shaft: at the midpoint and at the end of the rotor (*S1* and *S2* in Figure 4). The electromagnetic actuator was located at the non-drive end of the rotor; the armature corresponded to *Disk 3* in Figure 4. The electromagnetic actuator was controlled by an integrated digital signal processor and power amplifier unit. [16].

Figure 4. The rotor layout: the displacement sensors at "S1" and "S2" the actuator at "A". The dimensions are in millimeters.
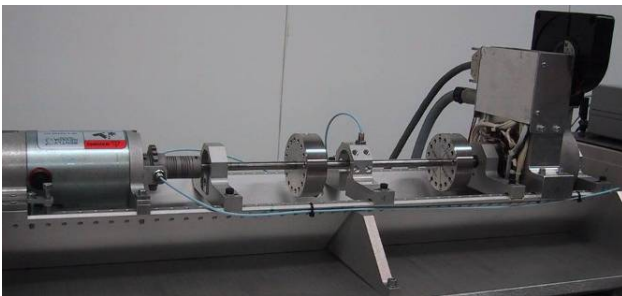

Figure 5. The driving motor (left), the rotor with the disks, and the actuator (right).

Three lowest natural vibration modes of the rotor shaft were identified experimentally (Figure 6). The corresponding natural frequencies were 46 Hz, 71 Hz, and 123 Hz in the horizontal plane and 46 Hz, 78 Hz, and 137 Hz in the vertical plane. The differences were caused by asymmetric rotor supports. To estimate frequency response functions, the rotor was excited with band-limited white noise (0…400 Hz) by the actuator. Responses were recorded at the sensor locations at different speeds of rotation. A simple Proportional-Derivative (PD) control was utilized during the identification of the responses. The proportional control produced an equivalent stiffness of 7 N/mm. The derivative part produced an equivalent damping of 43 Ns/m. In identification, the order of the dynamic model to be fitted was chosen as $m = 5$ (numerator) and $n = 6$ (denominator). Figure 7 and 8 show the least squares fits with the disturbance compensation method used in [16] in comparison with the direct Frequency Response Function (FRF) measurement without any disturbance compensation. The FRFs are shown from

the force commands to the rotor displacement. The identification results showed that the first resonance dominated at about 50 Hz. The next two modes at about 70–80 Hz and 120–140 Hz were weakly observable at the midpoint. This was due to the high damping and low displacement at the midpoint of those modes. The phase curves, however, indicate the existence of the modes.
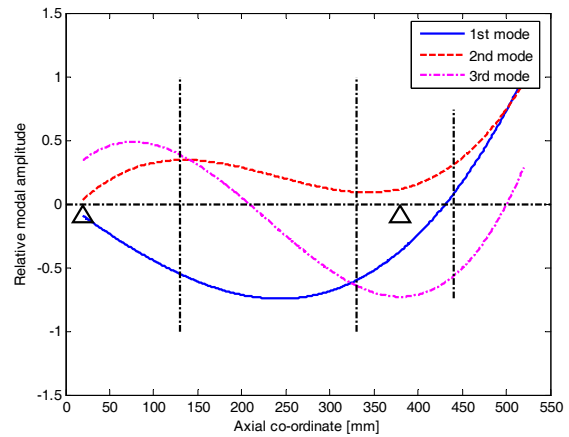

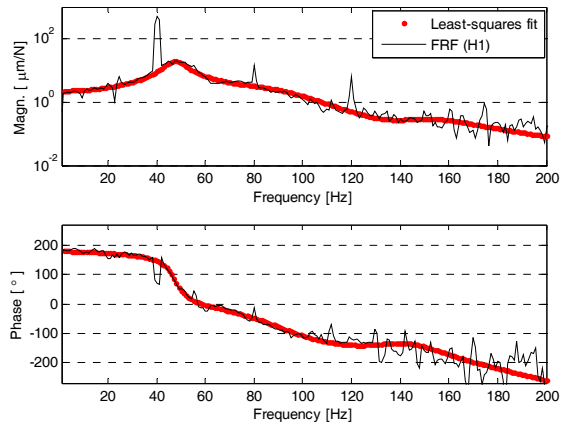Figure 6. The three lowest mode shapes of the rotor.

Figure 7. The FRF from the actuation point to the rotor midpoint when running at 40 rps.
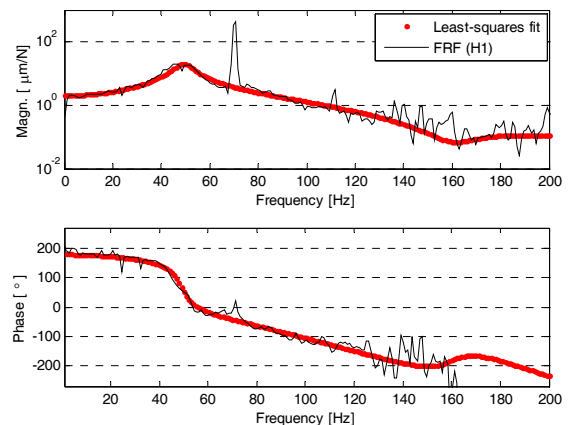

Figure 8. The frequency response function from the actuation point to the rotor midpoint when running at 70 rps.

In addition to repetitive learning control PD controllers together with an averaging low-pass filter were used in the feedback system. The transfer function from the displacement at the rotor endpoint to the force at the actuator is

$$H_{FB}(q) = \left(\frac{K_D}{T_S}\left(1 - q^{-1}\right) + K_P\right)\frac{1}{2}\left(q^{-1} + 1\right) \quad (5)$$

where K_D is the derivative gain, K_P is the proportional gain, T_S is the sample time, and q^{-1} is unit delay with length of T_S. The PD controller was mainly derivative in order to increase the damping of the system. The proportional term was minimal, because a load-carrying effect was to be avoided. The actuator was to have a minimal effect on the stiffness of the rotor. However, a light proportional control was utilized to generate a light centering force at a relatively flexible overhanging rotor end [16].

2.2 Gradient-Based Repetitive Learning Controller

The starting point for the development of a repetitive controller with adaptive delay time is the gradient-based method whose feedback path consisted of a truncated Finite Impulse Response (FIR) filter that had inverse phase behavior with respect to the actual plant. The behavior is obtained by using the time-inversed impulse response of the plant as the FIR filter [10]. This particular approach is selected because it is considered a computationally inexpensive method, possible to implement in the control unit. Also, its stability is guaranteed by sufficient model accuracy; sufficient modeling accuracy again meaning a phase error of ±90° [10]. Another way to examine the stability is to study destabilizing effects due to the FIR truncation, similar to the leakage phenomena in data acquisition [1]. Chen & Longman showed the existence of these effects and applied certain windowing techniques for repetitive control to avoid them [1]. Both approaches lead to a somewhat similar result requiring the modeling accuracy to be sufficient.

The idea is to use a pre-filter $K(q)$ that makes the loop gain positive real. In the current work, this is realized with a non-causal filter derived from the plant model.

$$K(q) = \alpha G_m(q) \quad (6)$$

where α is a real-valued convergence coefficient and $G_m(q)$ is the non-causal FIR model of the plant $G(q)$ where variable q is substituted by q^{-1}. The plant is approximated by a time-reversed truncated FIR model

$$G_m(q) = a_M q^M + a_{M-1} q^{M-1} + ... + a_1 q + a_0, M \leq N \quad (7)$$

where $[a_M ... a_0]$ are the FIR coefficients and M is the order of the FIR filter. The causality of the control law is guaranteed by truncating the FIR filter (restricting the order M) and by implementing it together with the delay line. Hence, the FIR length must be lower or equal to the

delay filter length in order to ensure the causality of the algorithm. As many FIR coefficients are chosen for the approximation as the delay filter length allows. Then, the FIR approximation is formed by flipping the truncated impulse response in the inverse order. The resulting filter has amplitude characteristics similar to the original plant (within the accuracy of the approximation). The phase characteristics of the FIR are inversed with respect to the plant. A phase lag in the plant corresponds to a phase lead in the FIR filter, and vice versa. With the truncated FIR, the control law becomes [10, 16, 17]

$$u(n) = q^{-N}\left(Q(q)u(n) + \alpha G_m(q)e(n)\right) \quad (8)$$

Similarly to the FIR approximation, the Q *filter* can be non-causal alone without the time delay. A symmetric filter can be applied

$$Q(q) = \\ c_P q^{-P} + c_{P-1} q^{-P+1} + ... + c_0 + ... + c_{P-1} q^{P-1} + c_P q^P, P \leq N \quad (9)$$

where $[c_P ... c_0]$ are the FIR coefficients and P is the order of the filter. The filter works usually as a low-pass or as a band-pass filter, but with zero phase lag. Although the pre-filters $Q(q)$ and $K(q)$ (or $G_m(q)$) may contain non-causal components, the control law itself remains causal if the orders of the filters are lower than the order of the time delay. The shown realization of the Q *filter* makes it a filter without phase lag. In other words, the frequency response of the filter is always real-valued

$$\text{Re}\left(Q(e^{i\omega'})\right) = Q(e^{i\omega'}), \\ \text{Im}\left(Q(e^{i\omega'})\right) = 0, \forall \omega' \in \begin{bmatrix} 0 & 2\pi \end{bmatrix} \quad (10)$$

where ω' is a normalized angular frequency in $[0, 2\pi]$.

2.3 Convergence to Zero Error

Algebraic examination shows how the repetitive control algorithm rejects a periodic disturbance. The result can be expected intuitively because the high (infinite) gain at the frequencies determined by the time delay provides a good disturbance rejection at those frequencies. However, the analysis below provides an algebraic insight in repetitive and iterative learning control methods.

Consider a polynomial $D(q)$ that works as an annihilator [13] (or an internal model by [2]) for a periodic disturbance signal $d(n)$

$$D(q)d(n) = \left(1 - Q(q)q^{-N}\right)d(n) \\ = d(n) - Q(q)d(n-N) = 0 \quad (11) \\ d(n) = d(n-N)$$

if $\text{abs}(Q) = 1$ and the period of the disturbance is N samples. The output of the plant $y(n)$ and the output of the repetitive controller $u(n)$ can be expressed as

$$y(n) = G(q)u(n) \\ u(n) = q^{-N}\left(Q(q)u(n) - \alpha G_m(q)e(n)\right) \quad (12)$$

Hence, the plant output can be expressed by

$$y(n) = G(q)\frac{-q^{-N}\alpha G_m(q)}{D(q)}e(n) \qquad (13)$$

Then, consider the control error

$$e(n) = y(n) + d(n) = d(n) - \frac{q^{-N}\alpha G_m(q)G(q)}{D(q)}e(n) \qquad (14)$$

Multiplication by the stable polynomial $D(q)$ gives

$$D(q)e(n) = D(q)d(n) - q^{-N}\alpha G_m(q)G(q)e(n) \qquad (15)$$

As noted above, the term $D(q)d(n) = 0$ if abs$(Q) = 1$.

$$\begin{aligned}\bigl(D(q) + q^{-N}\alpha G_m(q)G(q)\bigr)e(n) = 0 \\ \bigl(1 - q^{-N}Q(q) + q^{-N}\alpha G_m(q)G(q)\bigr)e(n) = 0\end{aligned} \qquad (16)$$

This shows that the disturbance signal is annihilated and the control error converges to zero with given assumptions.

2.4 Stability of Repetitive Learning Control

The pulse transfer function from the disturbance to the control signal of the gradient-based repetitive controller presented above becomes

$$H_r(q) = \frac{u(q)}{d(q)} = \frac{-q^{-N}\alpha G_m(q)}{1 - q^{-N}\bigl((Q(q)) - \alpha G_m(q)G(q)\bigr)} \qquad (17)$$

By using the *small gain theorem* (see *e.g.* [4]), the stability boundary for the system is

$$\begin{aligned}\left| e^{iN\omega'}\bigl(Q(e^{i\omega'}) - \alpha\overline{G}_m(e^{i\omega'})G(e^{i\omega'})\bigr) \right| < 1 \\ \left| Q(e^{i\omega'}) - \alpha\overline{G}_m(e^{i\omega'})G(e^{i\omega'}) \right| < 1, \forall \omega' \in \begin{bmatrix} 0 & 2\pi \end{bmatrix}\end{aligned} \qquad (18)$$

If we assume $Q(q) = 1$ for all the frequencies, and if the plant model perfectly describes the system (*i.e.* $G_m(q) = G(q)$), we have the stability condition for the convergence coefficient, or the learning gain

$$0 < \alpha < \sup\left(\frac{2}{\left|G(e^{i\omega'})\right|^2}\right), \forall \omega' \in [0, 2\pi] \qquad (19)$$

This result is derived by [10]. The result can be considered conservative, since the requirement concerns all the frequencies.

The truncation of the filter raises questions about the accuracy of the approximation and possible leakage effects due to the truncation. In practice, $G_m(q) \neq G(q)$, because of the truncated FIR approximation. According to the example in [1], the plant may be presented by two components, the actual model part and the residual part. Let the plant frequency response be

$$G(e^{i\omega T_S}) = G_m(e^{i\omega T_S}) + G_r(e^{i\omega T_S}) = \sum_{i=0}^{M-1} h_i e^{-i\omega T_S i} + \sum_{i=M}^{\infty} h_i e^{-i\omega T_S i} \qquad (20)$$

where $G_r(e^{i\omega T_S})$ is the residual part not included in the plant model, of order M. The FIR coefficients of the frequency response are represented by h_i. The model and the residual parts describe the system perfectly. In other words

$$G(e^{i\omega'})\bigl(\overline{G}_m(e^{i\omega'}) + \overline{G}_r(e^{i\omega'})\bigr) = \left|G(e^{i\omega'})\right|^2, \forall \omega' \in \begin{bmatrix} 0 & 2\pi \end{bmatrix} \qquad (21)$$

$\overline{G}_m(e^{i\omega'})$ and $\overline{G}_r(e^{i\omega'})$ are the complex conjugates of the plant model and the residual term. Stability analysis is based on the small gain theorem to limit the loop gain below unity and to obtain a sufficient condition for stability by this way [1]. The terms of Eq. (21) may be examined graphically on the complex plane where $-\alpha|G|^2$ represents the desired coefficient update and $-\alpha\overline{G}_m G$ represents the realized coefficient update. If the realized coefficient update does not stay within the unit circle, the algorithm is under a risk of instability. Figure 9 shows two imaginary scenarios for the significance of the residual term: a) the residual term does not have an effect and the system is stable, and b) the closed-loop system can be unstable without the residual term.
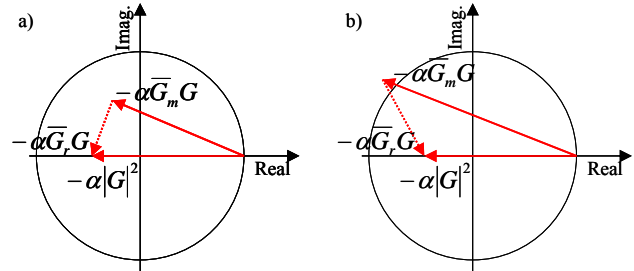

Figure 9. The illustration of the ideal, the plant model, and the residual gain vectors within the stability limits represented by the unit circle. Situation a) is acceptable. Situation b) where the residual vector contains stabilizing components should be avoided.

If we use the plant and the residual to describe the model, we can estimate their contribution to the stability. The substitution

$$G_m(e^{i\omega'}) = G(e^{i\omega'}) - G_r(e^{i\omega'}) \qquad (22)$$

modifies the stability condition into

$$\left| Q(e^{i\omega'}) - \alpha\bigl(\overline{G}(e^{i\omega'}) - \overline{G}_r(e^{i\omega'})\bigr)G(e^{i\omega'}) \right| < 1, \forall \omega' \in \begin{bmatrix} 0 & 2\pi \end{bmatrix} \qquad (23)$$

Examination of the complex vectors shows that the plant contains all the frequency components whereas the residual vector contains only the high frequency components (the minimum frequency being determined by $\omega T_S M$). The residual vector spins rapidly with respect to the plant vector in the complex plane, because it contains those high frequency components. To keep on the safe side, we may require that the plant vector is never closer to the unit

circle than the maximum length of the residual vector. Requiring

$$\left| Q(e^{i\omega'}) - \alpha \left| G(e^{i\omega'}) \right|^2 \right| < 1 - \alpha \left\| \overline{G}_r(e^{i\omega'}) G(e^{i\omega'}) \right\|, \forall \omega' \in \begin{bmatrix} 0 & 2\pi \end{bmatrix} \quad (24)$$

makes the stability limits conservative. In [1], norm $\left\| \overline{G}_r(e^{i\omega'}) G(e^{i\omega'}) \right\|$ was used in the equation above. This action was done in order to keep safe side in the stability analysis. As explained before, the residual term with high-frequency components spins rapidly in the complex plane.

The practical difficulty is that the true transfer function of the plant is usually unknown. Thus, the exact residual term is also unknown. The situation is shown graphically in Figure 10. The condition indicates a fundamental problem: if $\left| Q(e^{i\omega'}) \right| = 1$ and $\left| G_r(e^{i\omega'}) \right| > \left| G(e^{i\omega'}) \right|$, a small positive stabilizing α does not exist. On the other hand, this means that the loop gain is not positive real.
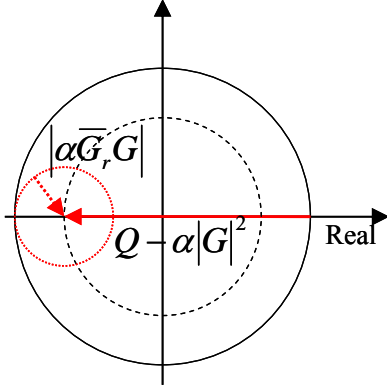

Figure 10. The graphical interpretation of the criteria in Eq. (24).

In [1], different windowing techniques were compared to be used together with truncation; the conclusion was to use exponential, and accelerated exponential, windows. Effectively this means using a frequency-dependent complex convergence coefficient (α) that corrects the loop gain in such a way that its positive realness is maintained. The criterion for evaluating the windows is the stability of the algorithm. Again, the conclusion is that stability is maintained if the truncated FIR model is capable of describing the phase within ±90° corresponding to the result derived in [10].

As the discussion shows, stability problems may occur at high frequencies if the residual term dominates. Besides windowing, another option is to use the *Q filter* to restrict the control action at high frequencies. Several windowing techniques have been proposed for FRF estimation in dynamic systems. Those techniques are aimed at preventing the leakage that is the generation of high-frequency components, from corrupting the result. Similar problems can occur with a truncated FIR repetitive controller [10].

2.5 Novel Repetitive Controller with Adaptive Delay Time

The update scheme for the truncated-FIR repetitive controller is

$$u(n) = q^{-N}(\gamma Q(q)u(n) - \alpha G_m(q)e(n)) \quad (25)$$

where $G_m(q)$ is the model of the system represented as a truncated FIR approximation of the system $G(q)$ and γ is a scalar leakage coefficient, less or equal to unity. The system model alone is a non-causal filter. However, the algorithm is causal, because the order of the FIR model does not exceed the delay length N.

The delay time has to be adjusted according to the speed of rotation. For variable-speed rotating machines, the delay time must thus be adjustable. Another option is to use the rotation phase-based delay, as in [3]. The solution makes it possible to use a constant delay, typically one revolution, *i.e.* 2 π rad. However, this experimental work exploited time-based repetitive algorithms [16, 17]. The choice was justified by two technical facts: 1) The measurement of the phase signals was not considered sufficiently reliable and accurate compared with the signal processor's capability of maintaining constant sampling intervals, and 2) The technical restrictions made it difficult to trigger the signal processing based on the rotor revolution pulses.

In the algorithm presented, the filter length is selected on-line according to the rotation speed estimation. The fundamental period of the disturbance is then determined by the rotation speed. The integer number of samples required is always rounded downwards to the nearest integer below by the algorithm

$$N = \text{floor}\left(\frac{1}{f_{rot}T_S} \right) \quad (26)$$

where f_{rot} is the measured speed of rotation. The fact that the required delay does not exactly meet the integer number of samples is taken into account by introducing a relative length error variable. The relative length error l_e between the realizable delay time and the required delay time is

$$l_e = \frac{1}{f_{rot}T_S} - N, \quad 0 \le l_e \le 1 \quad (27)$$

The length error is then used for the interpolation of the new control output by using two successive old outputs $u(n–N)$ and $u(n–N–1)$. The control law then becomes

$$u(n) = q^{-N}\left((1 - l_e + l_e q^{-1})u(n) - \alpha G_m(q)e(n) \right) \quad (28)$$

and the pulse transfer function from the disturbance to the control output equals

$$H_{ip}(q) = \frac{u(q)}{d(q)} = \frac{-q^{-N}\alpha G_m(q)}{1 - q^{-N}\left((1 - l_e + l_e q^{-1}) - \alpha G_m(q)G(q) \right)} \quad (29)$$

The interpolation is implemented in order have a more accurate frequency adjustment for the repetitive controller. Figure 11 shows the gain of the repetitive controller with

the interpolation feature in the vicinity of the first harmonic frequency. With the chosen parameters ($T_S = 0.0001$ s, $N = [20, 21]$, $l_e = [0, 0.25, 0.5, 0.75]$), the peak in the gain may be adjusted from 48.8 Hz to 51.1 Hz.
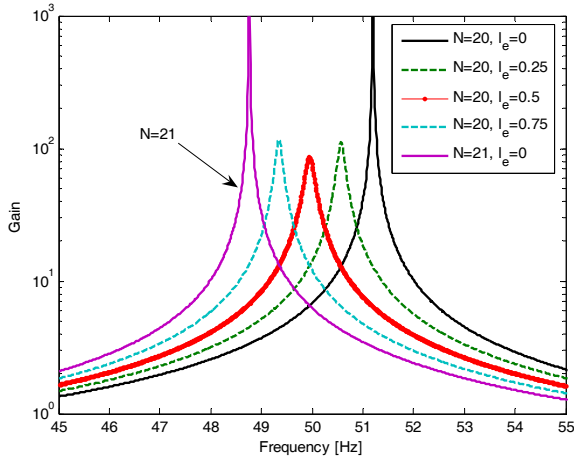

Figure 11. The gain of repetitive control loop as a function of frequency for different delay times (the filter order and the length error).

The interpolation, however, modifies the phase of the system and has a certain destabilizing effect. This feature diverges from the original idea of having a zero-phase system to ensure stability with high feedback gain [18, 9]. The issue is discussed below, after the completion of the algorithm used in the experimental work.

As explained above, the *Q filter* is used for limiting the frequency band of control actions. The type of *Q filter* used is a low-pass filter. A band-pass filter would have been required in order to avoid developing a DC component in control. The repetitive control method, being integrative, provides high feedback gain at zero frequency. It was, however, impossible to realize a sufficiently long and accurate band-pass filter due to technical restrictions of the control unit. Making an FIR-based band-pass-type *Q filter* that accurately has unity amplitude in the frequency band of interest requires a relatively high order filter. On the other hand, the maximum order of the filter is limited due to computational restrictions. Note that the *Q filter* alone does not require excessive computational power, but the overall algorithm using FIR representations for systems models, feedback control, and the DC removal feature presented below does. The computational cost of the algorithm increases rather rapidly.

This problem is avoided by implementing a separate DC removal system. The DC removal function is realized with a feedback of the integrated control signal. The transfer function of the feedback integrator alone equals

$$H_{in}(q) = \frac{1 - q^{-1}}{1 - q^{-1} - \omega_{LP}T_S} \quad (30)$$

where ω_{LP} is the integrator gain, used for the adjustment of the high-pass corner frequency. Finally, the control law,

shown in Figure 12, with adaptive delay time, interpolation, and the DC-removal function is expressed as

$$u(n) = \gamma q^{-N} Q(q)\left((1 - l_e) + l_e q^{-1}\right)u(n) + $$
$$- \alpha q^{-N} G_m(q)e(n) - \alpha\left(\frac{\omega_{LP}T_S}{1 - q^{-1}}\right)u(n) \quad (31)$$
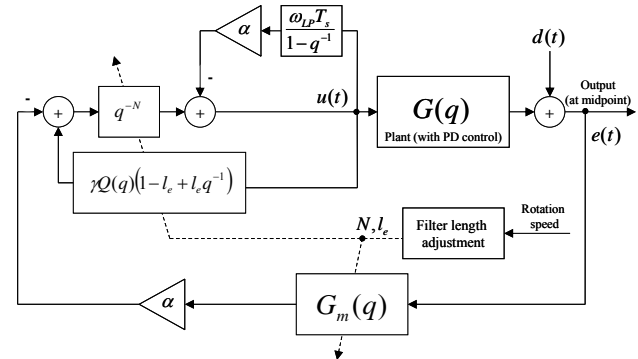

Figure 12. The repetitive control system applied to the test environment.

Similarly to the interpolation function, the DC removal function modifies the phase of the system and needs attention in terms of stability. The parameters γ and α determine the convergence and the stability properties of the algorithm. The pulse transfer function from the error signal to control output is

$$H_r(q) = \frac{-\alpha q^{-N} G_m(q)}{1 + q^{-N}\left(\alpha G_m(q)G(q) - \gamma Q(q)\left((1 - l_e) + l_e q^{-1}\right)\right) + \alpha\frac{\omega_{LP}T_S}{1 - q^{-1}}} \quad (32)$$

The system is time invariant for a constant rotation frequency, but N and l_e are updated according to the speed of rotation. Without the DC-removal integrator, $\gamma Q = 1$ and $l_e = 0$, the transfer function becomes

$$\frac{u(q)}{d(q)} = \frac{-\alpha q^{-N} G_m(q)}{1 + q^{-N}\left(\alpha G_m(q)G(q) - 1\right)} \quad (33)$$

Furthermore, if we assume that the model perfectly describes the system, we arrive at the stability condition stated earlier. If there are modeling errors, $\alpha G_m(q)G(q)$ becomes complex valued.

The next effort is to study the stability of the algorithm presented in Eq. (31) and shown in Figure 12. Multiplication by $(1-q^{-1})$ gives for the characteristic polynomial

$$P(q) = 1 - q^{-1} + (1 - q^{-1})q^{-N}\left(\alpha G_m(q)G(q) - \gamma Q(q)\left((1 - l_e) + l_e q^{-1}\right)\right) + \alpha\omega_{LP}T_S \quad (34)$$

The polynomial does not have a closed form solution for the roots. The interpolation feature induces a destabilizing component in the algorithms regardless the modeling error. A numerical examination shows that increasing the length error l_e pushes the high-frequency poles of Eq. (34) outside the unit circle (Figure 13).

Achieving stability requires the use of the *Q filter* for relative frequencies $\omega' > \pi/2$. The frequency limit is approximate and comes from a heuristic examination of the algorithm. The real part of term $\gamma Q(e^{i\omega'})((1-l_e)+l_e e^{-i\omega'})$ changes its sign $\omega' = \pi/2$ for $l_e = 1$. With the use of a low-pass type *Q filter* the poles remain inside the unit circle.
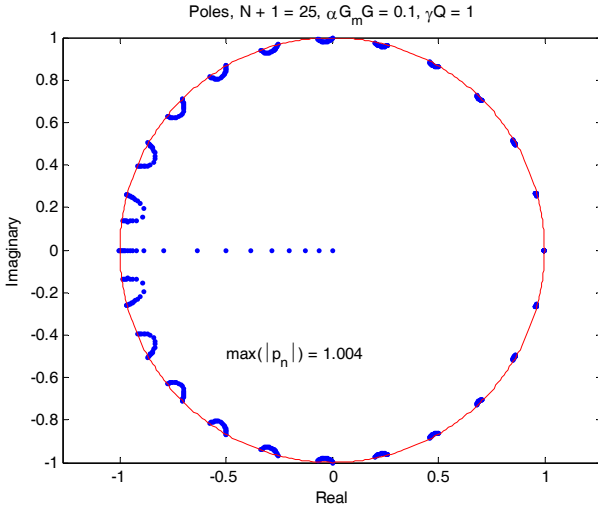

Figure 13. An example of the pole map of Eq. (34).

3.   EXPERIMENTAL RESULTS

The control algorithm presented in Eq. (31) was implemented on the rotor kit [16, 17]. As described above, the length of the delay time and the length of the FIR plant-model filters were adjusted according to the rotation speed estimation. The computational requirements of the algorithm and the performance of hardware caused restrictions on the operating range. A certain number of operations were available per signal processor cycle. The algorithm parameters were chosen such that the algorithm was operable at least in the vicinity of the rotor resonance at 50 Hz.

The maximum repetitive length selected was 35 (*i.e.* the FIR model order $N = 34$), and the minimum length was 15 ($N = 14$). These figures correspond to rotation speeds from 27 rps to 61 rps, for the implementation chosen. The FIR model filters were defined by impulse responses of the identified transfer functions in both planes separately. The FIR filters did not describe the system accurately, because relatively short filters were used. Figures 14 and 15 show comparisons of the longest and shortest FIR filters with the plant models. The implemented *Q filter* was a symmetric low-pass filter of length 15 (the current sample, 7 samples forwards and 7 samples backwards). Its –3 dB point lay at 240 Hz to limit high-frequency control actions. Standard filter design tools were utilized to compute the filter coefficients. An important aspect was to design a filter without overshoot in its frequency response. *Q filter*s with the same characteristics were implemented in both orthogonal planes (*X* and *Y*).
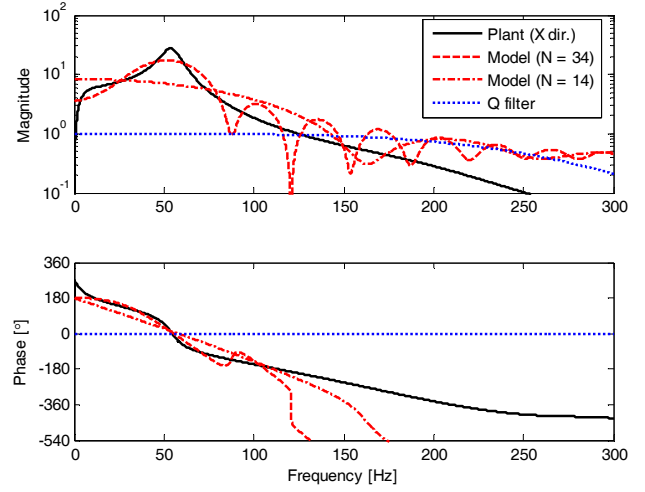

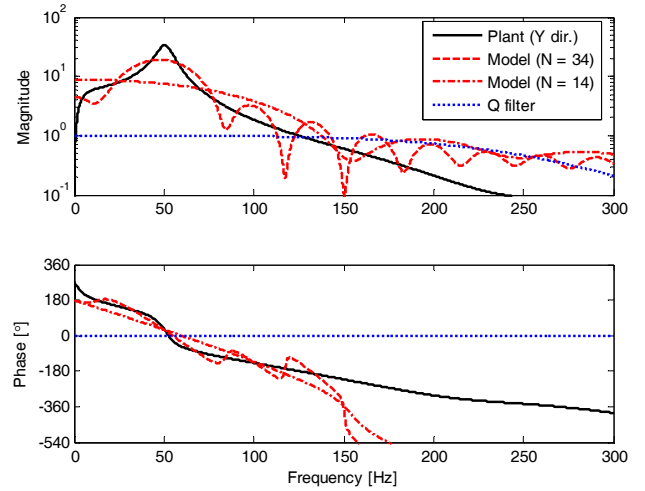Figure 14. The implemented filters in the X plane.

Figure 15. The implemented filters in the Y plane.

The feedback gain from the output error signal was influenced by the changing length of the plant-model filters. Figure 16 shows the effective repetitive feedback gains as a function of the repetitive filter length. The difference in the effective gains is caused by the different system models in the orthogonal directions. Figure 17 shows the open loop response for the complete repetitive control system from the control error $e(n)$ to the controller output $u(n)$.
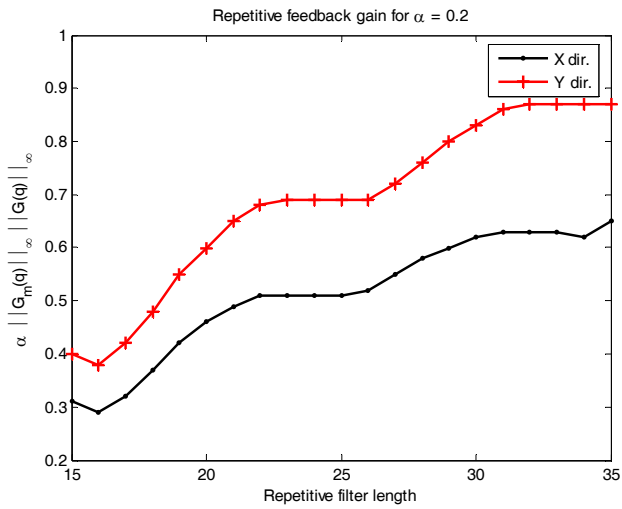
Figure 16. The feedback gain of repetitive control as a function of the filter length (delay time).
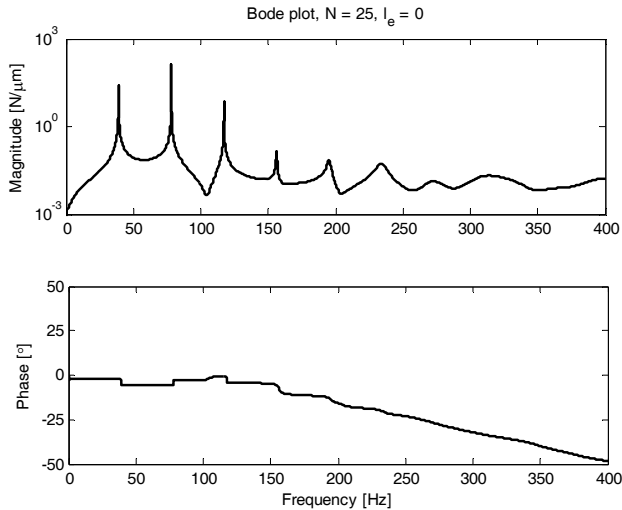

Figure 18. The rotor midpoint responses with repetitive control when running at 30 rps.

Figure 17. The open-loop response from the error to the repetitive controller output (computed for $\alpha = 0.1$, $N = 25$, and $l_e = 0$).

Figure 19. The rotor midpoint responses with feedback control, and with repetitive control when running at 40.7 rps. Speed matches with the filter length (24). $\alpha = 0.2$.

Figure 18 shows the rotor midpoint responses with the repetitive controller at a speed of 30 rps (revolutions per second). The damping achieved was 12 dB at the first and second harmonics. The response of the repetitive controller was found to be strongly dependent on the rotation speed. The performance was at its best when the disturbance period allowed an integer ratio between the required delay length and the sampling interval. In other words, the required delay time, stated by the rotation speed, was then realizable with an integer number of unit delays and the length error variable was close to zero. Later, the situation is called a match between the disturbance and the delay length. In this respect, the response plot shown did not present a good match between the disturbance and the delay length. Figure 19 shows the responses in case when the disturbance matches the delay length (40.7 rps).
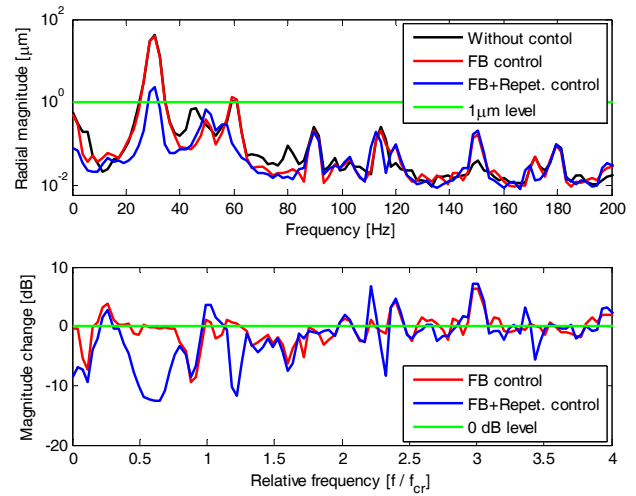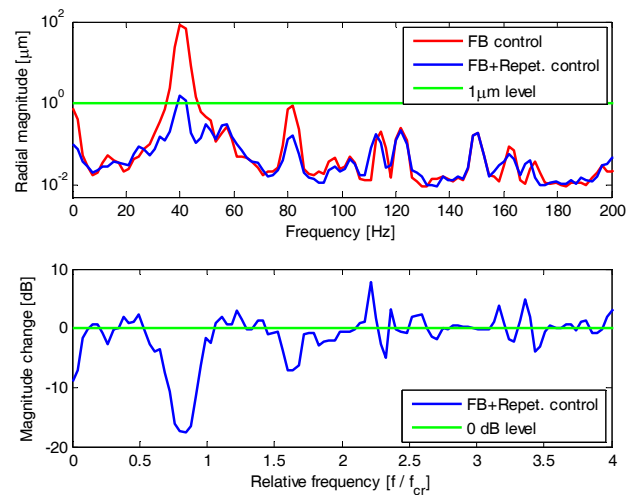
The algorithm was also run without *Q filter* for experimental purposes. The use of the filter with low-pass characteristics made the behavior of the algorithm substantially smoother.

For variable-speed experiments, the repetitive controller was tested in a rotor run-down condition (Figure 20). The run-down was performed from a rotation speed of 63 rps down to 32 rps with ramp rate of 4000 rpm/min (1.1 rps/s). The vertical dashed lines in the figure indicate the speed where the delay filter length matched the disturbance period. The local minima in the response did not occur exactly at the dashed lines, because of the transient (run down) operating condition. The figure shows that the performance was strongly frequency-dependent at high-speeds and the dependency weakened at lower speeds.
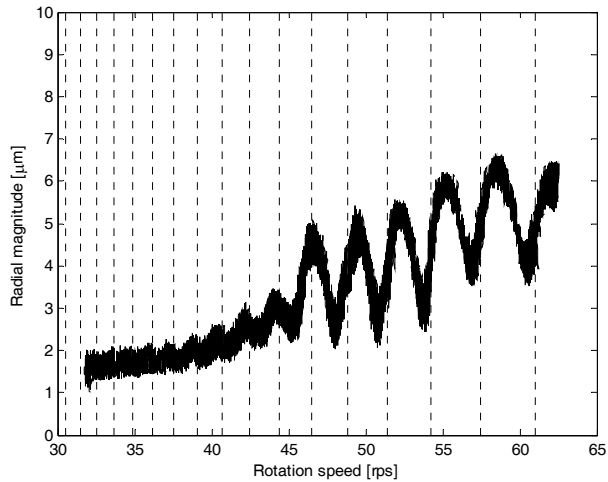
Figure 20. The radial displacement with repetitive control during a rotor run down (ramp rate equal to 4000 rpm/min).

4. CONCLUSIONS

The performance of the repetitive control method was at its best when the delay time matched the disturbance period. At those rotation speeds, the required repetitive length was realizable by an integer number of unit delays. Otherwise, the performance of repetitive control was poorer. The worsening of the performance can be understood by considering the integrative update law. A non-match situation causes a withdrawal of the integrator poles inwards from the unit circle. The situation is equivalent to a leaking integrator in the update law (parameter $\gamma < 1$).

The performance of the repetitive controller was relatively good for higher delay filter lengths ($N > 22$). For lower lengths ($15 < N < 22$), the performance became more dependent on the match between the disturbance period and the delay filter length. This was suspected to be caused by worsened plant model accuracy. The plant model accuracy was a function of the disturbance period, because the delay filter determined the maximum time-reversed FIR filter length. Using higher-order filters would have given smaller unit delays in the algorithm implementation.

Interpolation was used in the repetitive control law in order to provide a better match with the excitation frequency. This feature improved the performance. On the other hand, the same feature introduced a destabilizing term at high frequencies. The final form of a good way to formulate the interpolation may still need to be studied.

The tests presented did not do full justice to the repetitive control method's ability to track any periodic disturbance matching the delay time (of course, limited by the *Q filter* characteristics). In certain rotating machines, the frequencies of the most significant excitations may not be predictable. For example, rolls working in a nip contact may develop different barring vibration frequencies. These kinds of applications are good candidates for repetitive control.

The update law presented is not normalized to provide constant convergence over the operating range. Furthermore, the effective feedback gain changed as a function of the FIR model length. These features make the adaptation of the repetitive controller heavily dependent on the operating point.

In the current application, a rotation-phase based implementation such as proposed in [3] would probably have provided a better performance, but was not realizable for technical reasons. Sahinkaya *et al.* [14] applied a similar control method to repetitive control in order to update Fourier coefficients in the control of harmonic vibrations in magnetic bearing systems. This kind of mixed approach was not considered.

It is noteworthy that the repetitive controller worked at a relatively low system order and still provided a significant amount of attenuation. A straightforward way to improve the performance of the repetitive controller is to shorten the unit time delay used in the algorithm. In this way, the average mismatch between the disturbance period and the delay filter length is reduced. The plant model order, and thus the modeling accuracy, are also increased by the same modification. Hardware restrictions, however, did not allow testing the modification in the present test environment.

The repetitive controller presented was also compared with other feedforward-type mass unbalance compensation algorithms [16]. Those feedforward algorithms indicated better performance with the test rig studied.

Currently, research is directed towards active control of electrical machine vibrations using the machine's internal forces. The repetitive control method may be particularly useful, if periodic electromechanical excitations occur at unpredictable frequencies. Then, the repetitive controller must be implemented with a higher order algorithm than that in the current work. Moreover, the test environment probably poses new challenges for active control in the form of non-linear force generation. Furthermore, the stability condition derived for basic repetitive control algorithm was conservative and no analytical stability condition was derived for repetitive control with interpolation and DC removal. An effort is to study more precise and less conservative stability boundaries for the algorithms developed and to include modeling errors in the analysis.

REFERENCES

[1]   Chen K. & Longman R.W. *Stability issues using FIR filtering in repetitive control.* Advances in the Astronautical Sciences. Vol. 206. 2002. pp. 1321-1339.

[2]   Francis B.A. & Wonham W.M. *The internal model principle for linear multivariable regulators.* Appl. Mathematics & Optimization. Vol 2. No. 2 1975. pp. 170–194.

[3]   Fung R., Huang J., Chien C. & Wang, Y. *Design and application of continuous time controller for rotation mechanisms.* International Journal of Mechanical Sciences, Vol 42. 2000. pp 1805–1819.

[4]   Glad T. & Ljung L. *Control theory.* Taylor & Francis. London. 2000. 467 p. ISBN 0-7484-0878-9.

[5]   Hall S.R. & Wereley N.M. "Linear control issues in the higher harmonic control of helicopter vibrations". *Proc. of 45th Annu. Forum Amer. Helicopter Soc*. Boston, USA. pp. 955-971. 1989.

[6]   Hansen C.H. & Snyder S.D. *Active control of noise and vibration*, E & FN Spon, London, UK. 1997. 1267 p. ISBN 0-419-19390-1.

[7]   Hillerström G. *Active suppression of vibrations - a repetitive control approach*. IEEE Transactions on Control Systems Technology. Vol 4. No 1. 1996. pp. 72-78.

[8]   Hillerström G. & Sternby J. "Repetitive control using low order models". *Proc. of American Control Conference*. Vol. 2, 1994. pp 1873-1878. ISBN 0-7803-1783-1.

[9]   Hätönen J. *Issues of algebra and optimality in iterative learning control*. University of Oulu. 2004. 155 p. Doctoral dissertation. ISBN 951-42-7351-6.

[10]   Hätönen J.J., Freeman C.T., Owens D.H., Lewin P.L. & Rogers E. "Robustness analysis of a gradient-based repetitive control algorithm". *Proc. of 43rd IEEE Conference on Decision and Control*. Atlantis, Paradise Island, Bahamas. 2004. pp. 1301-1306.

[11]   Inoue T., Nakano M., Kubo T., Matsumoto S. & Baba H. "High accuracy control of a proton synchrotron magnet power supply". *Proc. of the 8th IFAC World Congress*. Vol. XX. Kyoto, Japan. 1981. pp. 216-221.

[12]   Kempf C., Messner W., Tomizuka M. & Horowitz R. *Comparison of four discrete-time repetitive control algorithms*. IEEE Control Systems Magazine. Vol. 13. 1993. pp. 48-54.

[13]   Medvedev A. & Hillerström G. "On perfect disturbance rejection". *Proc. of 32nd Conference on Decision and Control*. Vol 2. 1993. pp. 1324-1329. ISBN 0-7803-1298-8.

[14]   Sahinkaya M.N., Cole M.O.T. & Burrows C.R. "On the use of Scroeder phased harmonic sequences in multi-frequency vibration control of flexible rotor/magnetic bearing systems". *Proc. of the Eight International Symposiums on Magnetic Bearings*. Mito. Japan. Aug. 26-28, 2002. pp 217-222.

[15]   Smith C., Takeuchi K. & Tomizuka M. "Cost Effective Repetitive Controllers for Data Storage Devices". *Proc. of the 14th IFAC World Congress*, Beijing, China, July 1999.

[16]   Tammi K. *Active control of radial rotor vibrations – Identification, feedback, feedforward, and repetitive control methods*. Doctoral thesis, VTT Publications 634. Otamedia. Espoo. 2007. 151+5 p. ISBN 978-951-38-7007-2.

[17]   Tammi K., Hätönen J. & Daley S. *Novel adaptive repetitive algorithm for active vibration control of a variable-speed rotor*. Journal of Mechanical Science and Technology. The Korean Society of Mechanical Engineers. Vol. 21, Number 6. 2007. pp. 855-859. ISSN 1738-494X.

[18]   Tomizuka M., Tsao T.-C. & Chew K.K. *Analysis and synthesis of discrete-time repetitive controllers*. ASME Journal of Dynamic Systems, Measurement and Control. Vol. 111. 1989. pp. 353–358.

Kari Tammi received M.Sc. and Lic.Sc. degrees in mechanical engineering in 1999 and 2003 from Helsinki University of Technology, Finland. In 2007, he received D.Sc degree from the Department of Automation and Systems Technology at the same university. He has been with VTT – Technical Research Centre of Finland since year 2000. Currently, he is a Senior Research Scientist and Team Leader at VTT. The team named Electric Product Concepts is focused on machine and vehicle dynamics, modeling, simulation and control. In 2007–2008, he was a visiting post-doc researcher at North Carolina State University, Raleigh, USA. Prior to his position at VTT (1997 – 2000), he worked for CERN, European Laboratory for Particle Physics in Geneva, Switzerland.